Origin of the Distribution of Potential Barriers for Methyl Group Dynamics in Glassy Polymers: A Molecular Dynamics Simulation in Polyisoprene

F. Alvarez, A. Alegría, and J. Colmenero*

Departamento de Física de Materiales, y Centro Mixto CSIC-Universidad del País Vasco, UPV/EHU, Facultad de Química Apdo. 1072, E-20080 San Sebastián, Spain

T. M. Nicholson and G. R. Davies

IRC in Polymer Science and Technology, University of Leeds, Leeds LS2 9JT, U.K.

Received November 15, 1999; Revised Manuscript Received June 16, 2000

ABSTRACT: We have carried out molecular dynamics simulations of methyl group torsional librations in glassy polyisoprene at 150 K using the Insight and Discover codes from MSI Inc. with the Polymer Consortium Force Field. The model system was built using the MSI Amorphous Cell construction protocol with periodic boundary conditions. During the NVT molecular dynamics runs, the dihedral angle of each of the methyl groups and the positions of all of the atoms were recorded at 10 fs intervals. The results obtained support the generally assumed threefold approximation for the single particle methyl group potential. The density of states for methyl group torsional librations, as calculated from the time evolution of the dihedral angles, agrees quite well with previous inelastic neutron scattering results and shows a broad feature reflecting a distribution of potential barriers. This distribution is quantified in the framework of the threefold approximation. Performing similar simulations under different conditions for the nonbond interactions considered in the used force field, we conclude that the width of this distribution is mainly controlled by the nonbond interactions. Moreover, it turns out that these nonbond interactions also contribute significantly to the value of the average barrier for methyl group reorientation.

Introduction

Recent neutron scattering experiments of quantum and classical methyl group dynamics in glassy polymers have shown the significant role played by the distribution of potential barriers for methyl group rotation.[1−3] Due to the structural disorder inherent to the glassy state, the methyl groups in a glassy polymer have different local environments arising, in principle, from both the lack of regularity of the main chain conformation and the different local packing conditions. This manifests itself in a different mean field or single particle potential barrier for each rotating methyl group. The results from both quantum and classical temperature regimes of different polymers can be described consistently in the framework of the so-called rotation rate distribution model (RRDM) which was first proposed in 1994.[4] This model assumes a pure single particle threefold potential ($V(\varphi) = V_3(1 - \cos 3\varphi)/2$) for methyl group rotation, together with a Gaussian distribution of potential barriers $G(V_3)$. The distribution of V_3 yields distributions of the parameters driving the methyl group dynamics in both the classical and quantum regimes, namely, the activation energy for hopping through the barriers, the torsional libration levels, and the tunneling frequencies. These parameters can experimentally be obtained by means of neutron scattering spectroscopy[1−4] in particular. Although, as has already been mentioned, the origin of such distributions should be related to the structural disorder in general, their microscopic origin cannot be directly inferred from the experiments. Because of the fast time scale of methyl group dynamics, molecular dynamics (MD) simulation is a viable tool to gain insight into this problem. In particular, the calculation of the distribution of torsional librational frequencies for the methyl groups is quite straightforward and does not require lengthy molecular dynamics runs. It is worth emphasizing that, once this distribution is obtained, the corresponding distribution of threefold potential barriers can directly be inferred taking into account the relationship between torsional libration frequencies and the value of the corresponding V_3 potential barrier. In addition, MD simulations have the advantage that parameters defining the force field used in the simulations can easily be manipulated in order to investigate their influence on the methyl group dynamics.

In this work, we have carried out a MD simulation of methyl group torsional librations in glassy polyisoprene (PI). We have chosen PI because there are neutron scattering data for methyl group dynamics already reported in the literature[5] which allow us to validate our simulation results. Moreover, recent papers[6] show that realistic models of PI can be obtained by commercial force fields and well-established methods. As will be shown, we profited from the power of MD to simulate nonphysically attainable conditions such as "phantom chains" in order to throw light on the contributions made by intermolecular interactions to the distribution of barrier heights as compared with intramolecular interactions.

Model and Method

The simulations were carried out by using the Insight (Insight II 4.0.0 P version) and the Discover-3 programs from MSI[7] with the Polymer Consortium Force Field (PCFF). The model system used in these simulations was built using the Amorphous Cell module. The polymer system simulated was glassy polyisoprene (PI) as used in previous inelastic neutron scattering measurements.[5] Accordingly, the PI microstructure modeled was 90% of 1,4-PI (all the 1,4 units were chosen to be cis) and 10% of 3,4-PI. A cubic cell containing 3 PI-

10.1021/ma9919256 CCC: $19.00
Published on Web 09/23/2000

chains of 10 monomer units each was constructed at a density of 0.96 g cm^{-3} and at a temperature of 298 K. Such a density leads to a cubic cell dimension size of 15.5 Å. Periodic boundary conditions were assumed in order to model the bulk system, and for computational efficiency, a cutoff was applied to nonbond interactions between atoms separated by more than 6 Å. (To avoid potential discontinuities, the pair potential was smoothly raised to zero over 0.5 Å.) The 6 Å cutoff was chosen to be smaller than half the edge of the cubic cell in order to avoid interactions between an atom and its "image" due to the periodic boundary conditions.[8] All molecular dynamics runs were performed at constant volume and temperature (NVT) using the Velocity Verlet integrator with a 1 fs time step and velocity scaling (temperature window of 10 K) for temperature control.

Five separate cells were independently built in this way to ensure that a range of conformations of the amorphous polymer were explored. Simulations of PI chains embedded in glassy benzene ("dilute solid solution") were also carried out for comparison. In this case, a system of a PI chain of 10 monomer units (chosen among the previously used ones) and 200 molecules of benzene was built, which corresponds to a "solution" of about 4 wt %. The density of this system was adjusted to the density of benzene (0.88 g cm^{-3}), which leads to a cubic cell dimension of 31 Å at 298 K. As in the case of the PI melt, periodic boundary conditions were used, and five different cells with different initial conditions were also considered.

The different cells so constructed were first energy minimized by following well-known procedures before running 500 ps of molecular dynamics to equilibrate the samples. It is worth emphasizing that the temperature initially considered (298 K) is about 100 K higher than the experimental glass transition temperature of the real PI samples, thus allowing these systems of relatively short chains to equilibrate in a short time scale. After this procedure, the system was suddenly quenched to the glassy state at a temperature of 150 K, similar to the temperature at which the reported neutron scattering measurements were carried out. The density of the system was then adjusted to the estimated density at 150 K by changing the cubic cell edge to 15.2 Å and correspondingly scaling all atomic coordinates. After a further equilibration period of 500 ps, to accommodate this change in density, the production stage MD simulations were run for 160 ps on each of the constructed cells. During the dynamics runs, the dihedral angle $\varphi(t)$ corresponding to each of the methyl group protons was recorded every 10 fs. This angle defines the rotation of a given methyl group proton in the plane perpendicular to the bond linking the methyl group to the rest of the molecule. To calculate this angle for each methyl proton, four consecutive atoms are selected in a row, being the methyl proton the last (or the first) one of them. The dihedral angle defines the angle between the plane which corresponds to the first three atoms and the one which is defined by the last three ones. In addition to the dihedral angle of any methyl proton, the coordinates of all the atoms in the simulated cells were also recorded at each step. Results corresponding to successive runs did not show any signature of aging of the simulated system.

To investigate the influence of the nature of the nonbond interactions on the results obtained, MD simulations were also run for different values of the nonbond interaction cutoff ranging from essentially zero ("phantom" chain conditions) to 6 Å. In the case of the phantom chain conditions, the duration of the dynamics runs was limited to 5 ps, which experience has shown is long enough to calculate the density of torsional librations of methyl groups. The range of cutoff was also extended to higher values by considering a bigger cell.[8] The way in which this larger cell was constructed consisted of the following: The final configurations corresponding to each of the three molecules inside four of the five cells previously considered were used in order to build a new cell consisting of these 12 molecules altogether. The Amorphous Cell facility was again used to arrange these molecules at the same temperature and at the same density which was previously used for the separate five cells, resulting in a cell size of 24.12 Å. This size is large enough to extend the cutoff values up to about 11 Å. The so-obtained new cell was equilibrated by running a 1 ns dynamics before running the 160 ps dynamics in which data were collected and analyzed again. Moreover, in order to check the influence of the method used for controlling the temperature, the 160 ps run was also repeated by using the same initial configuration of the system but with the Nosé-Hoover thermostat instead of the velocity scaling method. Both algorithms showed to perform equally well to keep the temperature constant (standard deviation of about 2%). The vibrational densities of states (see below) calculated out from both dynamic runs were undistinguishable within the accuracy of our simulations.

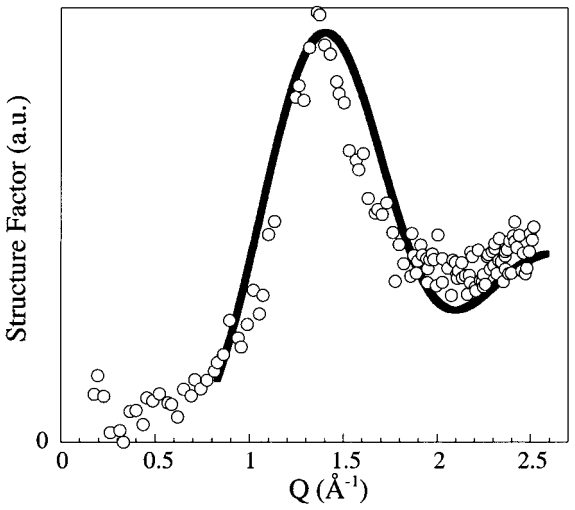

Figure 1. Static structure factor as measured by neutron scattering with spin polarization analysis in a protonated polyisoprene sample (circles) and as calculated from the MD simulations in this work.

To validate the structure obtained in the simulation cells, the neutron scattering static structure factor $S(Q)$ was calculated directly from the atomic coordinates by means of the following formula: $S(Q) \propto \sum_{j,k=1}^{n} f_j f_k \times \exp(i\vec{Q}\vec{r}_{jk})$, where the f_j stands for the atomic scattering factors for neutron radiation. We calculated $S(Q)$ from a large number of frames throughout the trajectories and averaged it. A similar calculation for a subsequent much longer (1 ns) dynamics run showed virtually the same result for the structure factor, thus giving confidence in the consistency of this result. The calculated $S(Q)$ was found to agree quite well with the experimental data measured with spin polarization analysis in the Q range from 0.5 to 2.5 Å^{-1} by means of D7 spectrometer (ILL, Grenoble)[9] as shown in Figure 1. This agreement

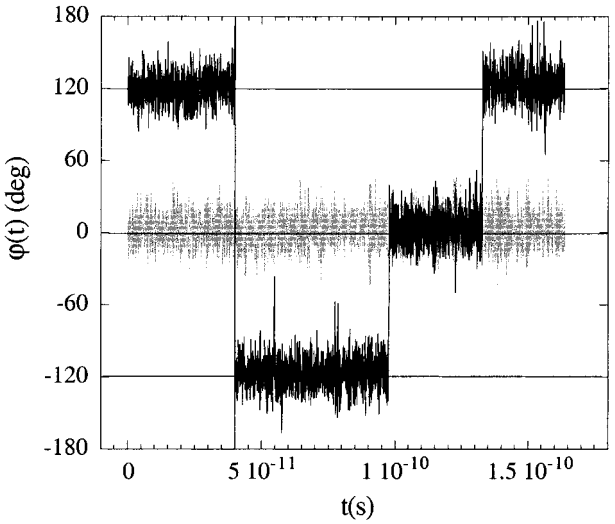

Figure 2. Time evolution of the dihedral angle, $\varphi(t)$, for two protons belonging to two different methyl groups chosen from the system.

validates the structure obtained in the simulation cells and gives support to the assumption that the simulations constitute a reliable mimic of the actual system, even if the simulated cells are rather small. The agreement found between the simulated and the experimental $S(Q)$ at the intermolecular level also indicates that the equilibration time used (500 ps) at 150 K is sufficient to accommodate the change in density from 298 to 150 K. On the othe hand, it is likely that this time does not allow the long-lenth scale conformational properties to equilibrate. However, in this work we are dealing with the very local side group motions that should not be very dependent on the overall chain dimensions.[10] For instance, in ref 6 it is reported that chain dimension seems to be not a critical parameter for local segmental dynamics in a polyisoprene model similar to that used in this work. As we will see below, for the kind of side group motions investigated in this work a more important criterion is the packing density and the intermolecular structure which are reflected in the first peak of $S(Q)$.

Results

At the low temperature of 150 K, most dihedral angles simply fluctuate around one of three states at approximately 0° or ±120°. However, some methyl groups also undergo a significant number of transitions among these states during the simulation runs. We have estimated that about 60% of the methyl groups only perform torsional librations during the simulation run (160 ps). An example of this behavior is shown in Figure 2 where it can be seen that, according to their different local conditions, one proton undergoes librations around a single equilibrium position while the other experiences transitions among three well-defined dihedral angles as the methyl group rotates. This can be taken as a first hint of the existence of some kind of distribution of potential barriers for methyl group rotation. The observed transitions would correspond to the lower barriers of the distribution.

These results seem to support the threefold jump model, which is usually assumed for analyzing neutron scattering data for classical methyl group rotation. To carefully check this question, we have calculated the dihedral angle distribution averaged over all the methyl group protons and trajectories for all the five cells. The results obtained are shown in Figure 3, which clearly indicates a threefold distribution. We have also calculated the distribution of the jumping angular amplitude, $\Delta\varphi$. This is defined as the change in the value of the dihedral angle of a given methyl proton when jumping between two well-defined equilibrium or stationary positions, averaged over all the methyl group protons which jump during the simulation runs. The resulting histogram is depicted in Figure 4 showing a narrowed peaked distribution centered on 120, thereby also in good agreement with the threefold approach. It is worth mentioning that previously reported simulations of poly(methyl methacrylate)[11] also agree with this conclusion.

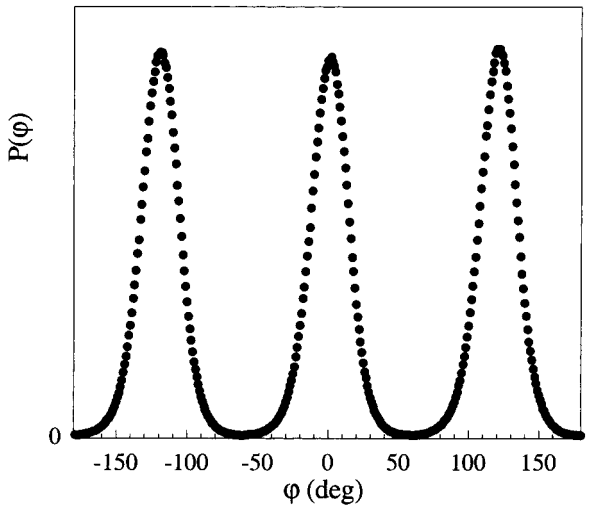

Figure 3. Dihedral angle distribution averaged over all methyl group protons and trajectories.

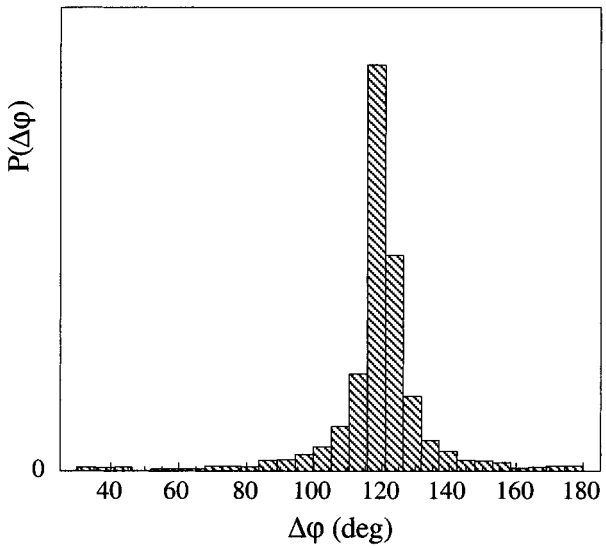

Figure 4. Distribution of the jumping angular amplitude, $\Delta\varphi$, averaged over all methyl group protons which undergo transitions during the dynamic runs.

From the MD simulation results the vibrational density of states (VDOS), $Z(E)$, can be calculated in general as the spectral density of the velocity autocorrelation function[12]

$$Z(E) \propto \int_{-\infty}^{\infty} e^{-iEt} \langle \mathbf{v}(0)\, \mathbf{v}(t) \rangle \, dt \qquad (1)$$

where the velocity autocorrelation function is calculated in terms of the velocity autocorrelation function of each

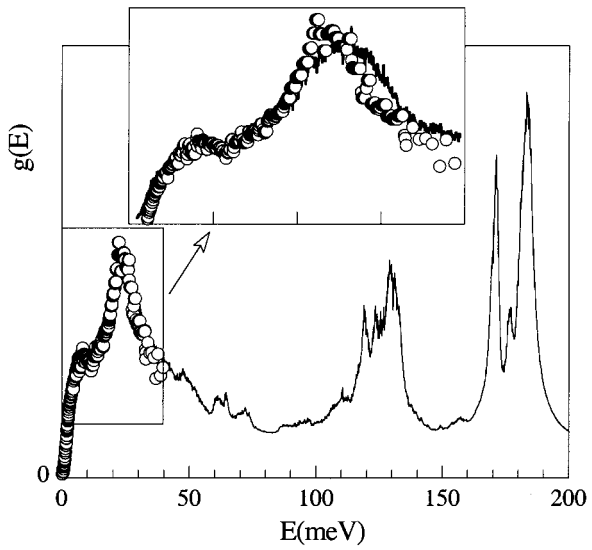

Figure 5. Vibrational density of states (VDOS) calculated for the methyl group protons in PI from MD simulations (solid line) and from neutron data (circles).

atom as

$$\langle \mathbf{v}(0)\ \mathbf{v}(t)\rangle = \frac{1}{N}\sum_i \langle \mathbf{v}_i(0)\ \mathbf{v}_i(t)\rangle \qquad (2)$$

and N is the number of atoms considered in the calculation. This approach was already used to characterize the vibrational properties of different molecular crystals (see as representative refs 13 and 14). Since in this work we are dealing with the vibrational properties of methyl groups in PI, we have calculated $Z(E)$ only for the protons of the methyl groups. The VDOS computed from the trajectories of the methyl group protons by using a numerical fast Fourier transform of the velocity autocorrelation (eq 1) is shown in Figure 5. The VDOS can also be evaluated from inelastic neutron scattering measurements by applying the incoherent Gaussian approximation.[5] Due to the high value of the incoherent scattering cross section of the proton (80.27 barns) as compared to its coherent cross section (1.76 barns) and to the cross sections of other typical nuclei in polymers (carbon, oxygen, deuterium, etc.),[15] the VDOS obtained from inelastic neutron scattering measurements in polymers corresponds to the subset of protons in the sample (hydrogen weighted VDOS). By means of the isotopic substitution technique (partial deuteration of polymer samples) the VDOS corresponding only to the protons in the methyl groups of PI can be measured using a PI sample where the protons of the main chain are replaced by deuterons. This was the procedure followed in ref 5, and the $Z(E)$ reported in that paper until about 40 meV is also included in Figure 5 for comparison. As can be seen in the figure, both the calculated from MD simulations and the experimental VDOS show a maximum around 25 meV, which in ref 5 was attributed undoubtedly to torsional librations of methyl groups. The magnification in the inset of the figure shows that there is a good agreement between the calculated and the experimental VDOS at least in the range of torsional librations where experimental data are available. This agreement indicates that both the average methyl rotational barrier and the distribution of potential barriers are well reproduced with the force field used. This again validates our MD simulations. On the other hand, the calculated $Z(E)$ from MD simulations also shows other maxima at higher energies which cannot be directly compared with inelastic neutron scattering results. However, although quantum effects certainly affect the high-energy range of $Z(E)$, the energies of the above-mentioned maxima roughly correspond to those of the different infrared bands associated with the methyl groups of PI (see for example ref 16). In particular, the energy of both the CH_3 umbrella deformation (~170 meV) and the CH_3 asymmetric deformation (~180 meV) bands seems to be well reproduced even though we are using classical methods of simulation.

It is worth emphasizing that although the $Z(E)$ shown in Figure 5 only corresponds to the methyl group protons, this function contains not only the torsional librational modes but also other vibrational contributions which, experimentally, cannot be easily separated without taking strong assumptions about the character of these modes. This is evident in Figure 5 where the torsional librational peak is superimposed in some way to a broad low-energy hump. However, once we have checked the good agreement between simulations and inelastic neutron scattering results, we can take advantage of the MD possibilities to isolate the torsional librational part from $Z(E)$. In the following we will call this part, i.e., the torsional libration density of states, as $g(E)$. This function is formally defined as the spectral density of the angular velocity correlation function:

$$g(E) \propto \int_{-\infty}^{\infty} e^{-iEt}\langle \dot{\varphi}(0)\ \dot{\varphi}(t)\rangle\, dt \qquad (3)$$

where

$$\langle \dot{\varphi}_i(0)\ \dot{\varphi}_i(t)\rangle = \frac{1}{N}\sum_i \langle \dot{\varphi}_i(0)\ \dot{\varphi}_i(t)\rangle \qquad (4)$$

and N is in our case the number of methyl group protons. To calculate $g(E)$ numerically, we have followed the following procedure based on a Fourier representation of the time evolution of the dihedral angles $\varphi(t)$. If $\dot{\varphi}(t)$ is expressed in terms of its Fourier components $\{B_n\}$ as $\dot{\varphi}(t) = \sum_n B_n \exp(iE_nt)$, then $g(E_n) \propto |B_n|^2$. The magnitude directly calculated from the MD simulations is $\varphi(t)$, which can easily be expressed in a Fourier representation as $\varphi(t) = \sum_n A_n \exp(iE_nt)$. It is elementary to show that $B_n = iA_nE_n$, and hence, the density of methyl group torsional librations can be calculated as $g(E_n) \propto |A_nE_n|^2$.

The results obtained by this procedure are shown in Figure 6 where $g(E)$ shows a broad feature reflecting a distribution of potential barriers for methyl group rotation in PI. The figure also shows the $g(E)$ obtained from MD simulations carried out in the "bigger cell" mentioned in the Model and Method section, but using the same cutoff value (6 Å) for the nonbond interactions used in the case of the five separated cells. As can be seen, both $g(E)$ functions are equivalent within the uncertainties involved. As it has already been mentioned, $g(E)$ cannot be directly obtained from the inelastic neutron scattering data which always measure the total hydrogen weighted VDOS called by us $Z(E)$. However, a rough estimation of $g(E)$ can also be evaluated from the experimental data by assuming that the additional modes contained in $Z(E)$, other than methyl group torsional librations, are similar to the modes of the protons in the main chain of the polymer. The latter

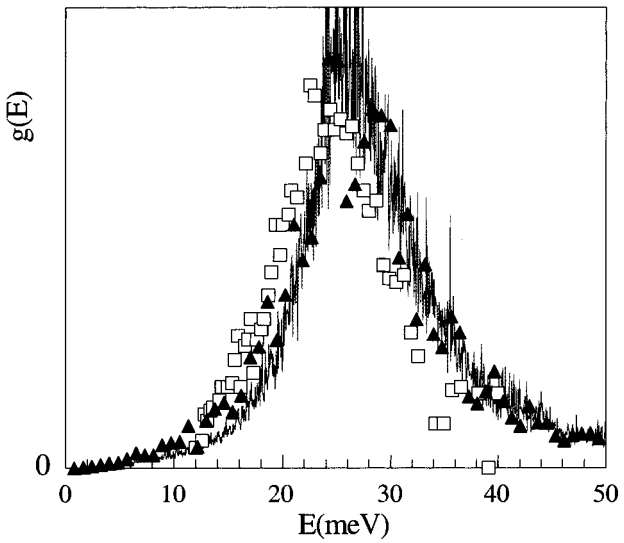

Figure 6. Distribution of the methyl group torsional frequencies of PI. The solid line and the filled triangles were obtained from MD simulations using a single big cell (solid line) and averaging over five small cells (triangles). The empty squares were estimated from experimental neutron data.

can be calculated from inelastic neutron scattering measurements carried out on a PI sample with the methyl group deuterated and the main chain protonated (more experimental details can be found in ref 5). Therefore, we have estimated the "experimental" $g(E)$ as the difference between the two hydrogen weighted VDOS shown in Figure 7 of ref 6, which correspond to a PI sample with the methyl group protonated and the main chain deuterated and to another PI sample with the methyl group deuterated and the main chain protonated. The so obtained $g(E)$ is also shown in Figure 6 for comparison. The agreement with the properly calculated $g(E)$ from MD simulation is quite reasonable although we have to point out, once again, that the so-called "experimental" $g(E)$ is only a crude estimation.

One of the main goals of this work is to calculate the distribution of potential barriers for methyl group rotation in glassy polyisoprene at 150 K: To do this, one of the most direct possibilities would be to compute a conformational state autocorrelation function taking into account the transitions between different dihedral states. This procedure is very suitable at high temperature where all the methyl groups carry out several transitions during the simulation run.[17] However, as has already been discussed, this is not the case at the low temperature (150 K) here investigated. In this low-temperature range, an indirect way based on the calculated $g(E)$ can be envisaged once the threefold approximation has been tested. In the framework of this approximation, we can easily transform the calculated $g(E)$ into the corresponding distribution of threefold potential barriers, $G(V_3)$ as $G(V_3) = g(E)\, dE/dV_3$. To do this, we need to establish a relationship between E and V_3. In the framework of a quantum picture, but assuming that the density of torsional states only corresponds to the first quantum librational state, a numerical relationship between the librational energy E and the potential barrier V_3 can be established from the solutions of the corresponding static Schrödinger equation. Tabulated solutions of this equation—which for a pure sinusoidal threefold potential takes the form of the well-known Mathieu equation—can be found for example in ref 18 for different values of the potential barrier V_3.

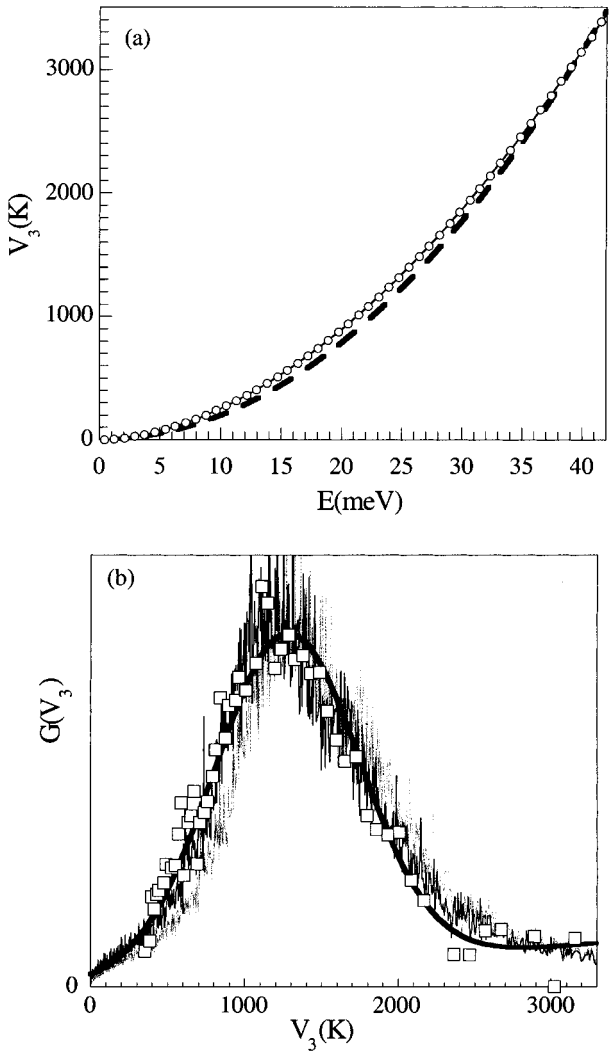

Figure 7. (a) Relationship between the 3-fold potential barrier, V_3 (K), and the energy of torsional librations, E (meV): (○) from the solution of the static Schrödinger equation and (- - -) from the harmonic classical approximation (see the text). (b) Distribution of potential barriers for methyl group rotation, $G(V_3)$, in polyisoprene obtained from the distribution of torsional libration frequencies, $g(E)$, by means of the relationships between E and V_3 shown in (a): (black line) harmonic classical relationship; (gray line) quantum relationship. The figure also shows the values of $G(V_3)$ obtained from the so-called "experimental" $g(E)$ by using the quantum relationship (empty squares). The thick curve is a fitting of the classical $G(V_3)$ to eq 5 in a range of V_3 up to 3500 K.

These numerical solutions allow one to correlate the values of V_3 and E. The correlation can be well described by a general power law like $V_3 \cong aE^{\alpha}$, where the values of the parameters a and α depend on the range considered. In the range of V_3 which is relevant for this work ($V_3 < 3500$ K approximately) the values found for these parameters are $a = 3.86$ and $\alpha = 1.82$ when V_3 is given in K and E in meV. The numerical correlation between E and V_3 as well as its description by the power law with such parameters is shown in Figure 7a in the mentioned V_3 interval. From this analytical function, dE/dV_3 and thereby $G(V_3)$ can easily be calculated. Figure 7b shows the distribution $G(V_3)$ obtained by means of this procedure from the $g(E)$ distribution corresponding to MD simulations. We have also followed this procedure to calculate an "experimental" $G(V_3)$ from the experimental estimation of $g(E)$. The resulting distribution is also included in Figure 7b.

The procedure described above is formally correct in terms of a quantum picture ("librational states") and thereby is the suitable procedure when one deals with actual inelastic neutron scattering data. However, it is worthy of note that in this work we are dealing with a classical MD simulation. Therefore, the calculated $g(E)$ from MD simulations should be better interpreted as a distribution of classical frequencies, which give the curvature of the librational well. In the framework of a simple harmonic approximation, it is straightforward to demonstrate that the harmonic frequency E is given by E (meV) $= (9V_3B)^{0.5}$, where $B = h^2/2I$ is the rotational constant of the methyl group ($B = 0.655$ meV) and I its moment of inertia. This finally gives $V_3 = 1.97E^2$ when V_3 is in K units and E in meV. This function is also plotted in Figure 7a for comparison with the quantum relationship discussed above. Figure 7b also shows the distribution $G(V_3)$ obtained from the $g(E)$ corresponding to the MD simulations but now calculated using the harmonic classical approximation. The so-obtained "classical" $G(V_3)$ is a little bit shifted toward lower energies with respect to the $G(V_3)$ function obtained in terms of the quantum picture. The difference between both distributions can be considered as the uncertainty limit of our procedure for obtaining $G(V_3)$. It is noteworthy that the "classical" $G(V_3)$ fits better the "experimental" $G(V_3)$ obtained from the experimentally estimated $g(E)$. In the following we will discuss our results in terms of the "classical" $G(V_3)$.

As was expected from the broad torsional libration $g(E)$ peak, the corresponding distribution function $G(V_3)$ also shows a broad feature with a maximum centered around 1200 K and a half-width at half-maximum (hwhm) of about 450 K. These values are typical of glassy polymers[2] and in agreement with quasielastic neutron scattering data for the same system.[19]

As mentioned in the Introduction, the distribution function $G(V_3)$ which is assumed in the RRDM is Gaussian. This symmetric shape has proved to be suitable for describing not only the high-temperature hopping processes of methyl groups in different polymers but also the low-temperature quantum tunelling processes[1,3] and the crossover from quantum to classical behavior as well.[20] However, the distribution $G(V_3)$ obtained here from the distribution of torsional librations has a certain asymmetry, showing a high-energy tail. This does not seem to be a consequence of the MD simulations, since, as Figure 6 shows, the so-called "experimental" $G(V_3)$ estimated from the inelastic neutron scattering data also displays the same tendency. In the case of the experimental data, this could be due to the fact that the $G(V_3)$ shown in Figure 7b was estimated by assuming that only the first libration state contributes to $g(E)$. It is clear that, at the temperature considered (150 K), this is only an approximation and transitions involving second and higher torsional excited states should contribute to the high-energy range of the estimated density of torsional states. However, this possible explanation does not apply in a classical dynamic simulation. The clarification of this point needs future experimental and MD simulation work in other polymers. In any case, Figure 7b shows that $G(V_3)$ can be well described in terms of a Gaussian distribution plus a linear term:

$$G(V_3) \propto \exp\left[-\frac{(V_3 - \langle V_3\rangle)^2}{2\sigma^2}\right] + c_1V_3 + c_0 \qquad (5)$$

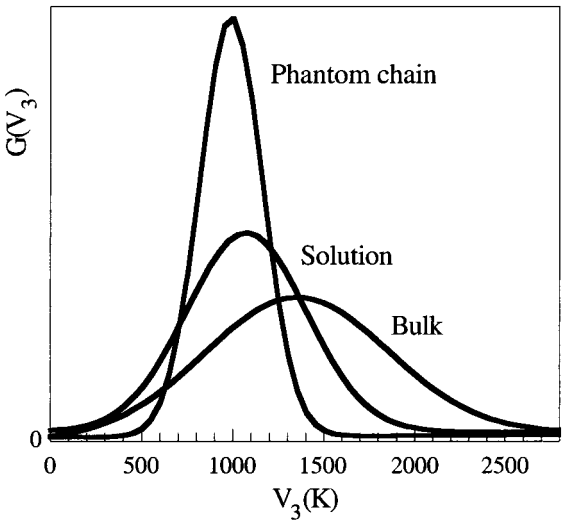

Figure 8. Distribution of potential barriers, $G(V_3)$, for methyl group reorientation in PI from MD simulations in the bulk, under phantom conditions, and in a "solid solution" of benzene.

with the following values of the parameters:

$$\langle V_3\rangle = 1276 \text{ K}, \quad \sigma = 470 \text{ K}, \quad c_1 = 3.59 \times 10^{-5}\,\text{K}^{-1}, \quad c_0 = 1.21 \times 10^{-2}$$

In the following we will represent $G(V_3)$ by means of this kind of functional parametrization, and we will discuss the results in terms of the two parameters of the Gaussian distribution.

Discussion

Neutron scattering results suggest[2] that the average value of the activation energy for the methyl group reorientation in glassy polymers is mainly driven by the chemical structure of the monomer and, in particular, by the position of the methyl group, i.e., whether it belongs to an ester group, whether it is directly linked to the chain, or whether it is located in a different environment. On the other hand, there is no clear dependence of the width of the distribution of potential barriers on the chemical structure. This suggests that this distribution may be controlled mainly by intermolecular interactions and packing conditions, which should, in principle, be rather similar for different polymer glasses.

We can take advantage of the possibilities of MD simulations to get some insight into this question. MD simulations allow easy monitoring of the contribution from the different terms affecting the dynamics. Furthermore, some energy contributions can even be eliminated from the system by just "switching off" the corresponding interactions, and then, by monitoring the subsequent dynamics under those conditions, one can study the effect of such a change on the dynamics of the system. For instance, by excluding the nonbond energy terms corresponding to van der Waals and Coulombic forces, from the total potential energy of the system (phantom-chain conditions), one can learn how this affects the results obtained for the distribution of potential barriers.

The result obtained for $G(V_3)$ under these phantom conditions is displayed in Figure 8. As can be seen, the maximum of $G(V_3)$ is now shifted toward lower energies,

indicating that the nonbond interactions significantly contribute to the single particle potential barriers for methyl group rotation. We can estimate a factor of about 1.5 between the average value of V_3 in the bulk and in the "phantom chain". Moreover, Figure 8 also shows that there is a strong narrowing of the distribution $G(V_3)$ when the nonbond interactions are switched off. We can estimate a factor of about 3 between the hwhm of $G(V_3)$ in the bulk and in the "phantom chain". This result clearly indicates that the microscopic origin of the width of $G(V_3)$ is directly related to the nonbond interactions. It is worthy of remark that qualitative similar results were obtained by a different MD simulation method[21] for the reorientation of a more complex side group: the ester group in methyl acrylate/ethylene copolymers. In this case, the ratios for the average barrier height and the hwhm were 1.6 and about 6, respectively.

On the other hand, it is worthy of note that, even for the phantom-chain conditions, the width of the distribution of potential barriers $G(V_3)$ obtained is nonzero. This could be, in principle, understood in terms of a narrow distribution of potential barriers associated with the bond interactions and thereby likely related to the lack of chain conformational regularity. However, it is noteworthy that this width could also be related—at least in part—to the anharmonicity of the threefold sinusoidal potential. If the potential is not perfectly harmonic, the frequency of the torsional librations depends on the amplitude of the oscillations. This implies that, even taking into account a single potential barrier, we would observe a distribution of harmonic torsional frequency of librations $g(E)$. This distribution of torsional frequencies will transform into an apparent distribution of potential barriers $G(V_3)$. Our simulation results seem to suggest this possibility because the distribution of torsional frequencies $g(E)$ calculated for only one methyl group shows, on average, a broadening of the order of the broadening of the phantom-chain distribution, though the statistics are very poor. The clarification of this point needs longer MD simulations—better statistics—and also to vary in a systematic way the different bond interactions which contribute to the force field. This is beyond the aim of this paper and will be the subject of future work. For the discussion of the results here obtained, we should consider the broadening of the phantom chain distribution as our "instrumental resolution".

Clearly, the "phantom-chain" condition can never be achieved experimentally. Therefore, it was desirable to check the effect of the nonbond interactions on methyl group dynamics in a more realistic system. To do this, we have constructed a system in which a PI chain is embedded in a solvent (benzene) at the same temperature of 150 K, previously used, for the sake of being able to compare the same dynamics of the chain when subjected to different environmental conditions. Nevertheless, we should be aware that, at this temperature, benzene is in a solid glassy state. The results obtained for $G(V_3)$ are also shown in Figure 8 for comparison with the bulk and "phantom-chain" results discussed above. As can be seen, in the case of solid solution conditions, we obtain an intermediate behavior. Further experimental work can thus be envisaged to test this prediction.

There is still a further step we can take in connection with the relationship between the origin and width of the distribution and the nonbond interaction terms of

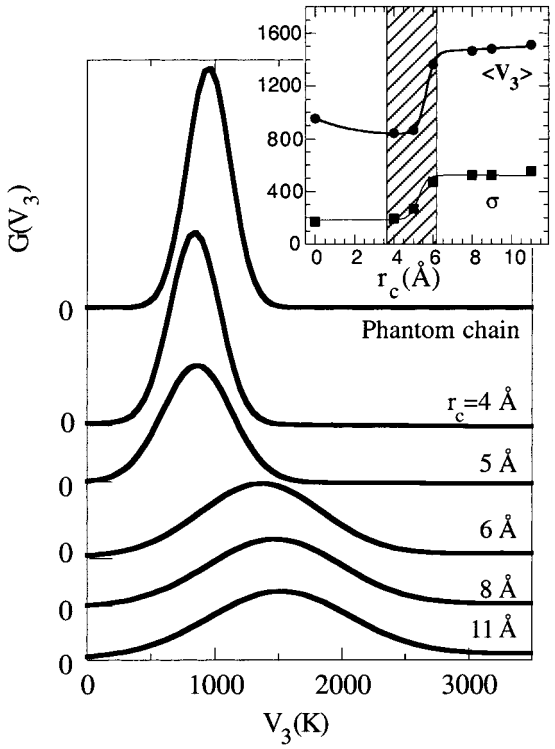

Figure 9. Effect of the cutoff value, r_c, for nonbond interactions on the distribution of potential barriers for methyl groups reorientation. The inset shows the evolution of the average potential barrier, $\langle V_3 \rangle$, and the width of the distribution, σ, with r_c.

the force field. Figure 8 suggests that softening of the nonbond interactions causes a decreasing of the energy corresponding to the maximum of the distribution peak and a narrowing of the distribution. The systematic nature of this trend was tested by running a series of MD runs with different cutoff for the nonbond interactions considered in the used force field. The way by which these simulations were carried out has already been described in the Model and Method section. It is worthy of remark, once again, that for the cutoff value of 6 Å the $g(E)$ obtained in the case of the "bigger cell" was equivalent to that obtained by using the average of the five smaller cells (see Figure 6). The results obtained by changing the cutoff value are shown in Figure 9. They confirm the systematic nature of the above-mentioned correlation. The inset of the figure displays the average value of V_3, $\langle V_3 \rangle$, and the width of the Gaussian distribution, σ, as a function of the cutoff value used. It is evident that the main changes take place in a narrow region around a cutoff value of 5 Å (see the shaded area in Figure 9). It is worthy of remark that these values are in the range of the correlation length $d = 2\pi/Q_{max}$ associated with the maximum of the static structure factor shown in Figure 1 and which corresponds to the interchain distances. This shows that only the nonbond interactions at the interchain distances seem to play a significant role in determining the width of the distribution of rotational barriers for the dynamics of the methyl group rotations in PI. Moreover, it is also worthy of note that these interactions also affect significantly the average value of the potential barrier; i.e., this is not only determined by the chemical structure of the monomer as it was in principle supposed from neutron scattering results.

Conclusions

We have constructed a MD simulation of a PI bulk system, which appears to be a reasonably realistic one in the sense that the calculation of its structure factor agrees with that experimentally measured by neutron scattering. Furthermore, the density of vibrational states for the methyl groups calculated from the simulated dynamics compares well with that obtained from previous experimental inelastic neutron scattering data. In this way, we have been able to check the threefold approximation for the single particle potential for methyl group reorientation in PI. We have also calculated the distribution of torsional librations of methyl groups and the corresponding distribution of threefold potential barriers. Moreover, we have profited from the versatility of MD simulations to investigate the origins of such distributions. We have shown that the width of the distribution of threefold potential barriers is related to the nature of the nonbond interactions at the interchain distances: the weaker the nonbond interaction, the narrower the width of the distribution. Finally, it is also shown that the nonbond interactions contribute significantly to the average barrier height for methyl group rotation.

Acknowledgment. F.A., A.A., and J.C. acknowledge the support given by the Spanish Ministry of Education (Project No. PB97-0638), the Government of the Basque Country (Projects No. PI-1998-20 and EX-1998-23), the University of the Basque Country (Project No UPV206.215-G20/98), Donostia International Physics Center, Gipuzkoako Foru Aldundia, and Iberdrola S.A. We also thank Dr. B. Frick for fruitful discussions.

References and Notes

(1) Colmenero, J.; Mukhopadhyay, R.; Alegría, A.; Frick, B. *Phys. Rev. Lett.* **1998**, *80*, 2350.
(2) Mukhopadhyay, R.; Alegría, A.; Colmenero, J.; Frick, B. *Macromolecules* **1998**, *31*, 3985.
(3) Moreno, A.; Alegría, A.; Colmenero, J.; Frick, B. *Phys. Rev. B* **1999**, *59*, 5983.
(4) Chaid, A.; Alegría, A.; Colmenero, J. *Macromolecules* **1994**, *27*, 3282.
(5) Frick, B.; Fetters, L. J. *Macromolecules* **1994**, *27*, 974.
(6) Moe, N. E.; Ediger, M. D. *Polymer* **1996**, *37*, 1787 1996; *Phys. Rev. E* **1999**, *59*, 623.
(7) Molecular Simulations Inc., San Diego.
(8) Due to the use of periodic boundary conditions, the Lennard-Jones cutoff distance used in the MD simulations should be smaller than half of each one of the three edge lengths of the simulation box (see, e.g.: Allen, M. P.; Tildesley, D. J. *Computer Simulation of Liquids*; Oxford University Press: New York, 1997).
(9) Alvarez, A.; et al., to be published.
(10) Clarke, J. H. R. In *Monte Carlo and Molecular Dynamic Simulation in Polymer Science*; Binder, K., Ed.; Oxford University Press: New York, 1995.
(11) Nicholson, T. M.; Davies, G. R. *Macromolecules* **1997**, *30*, 5501.
(12) See, e.g.: Egelstaff, P. A., Ed.; *An Introduction to the Liquid State*; Oxford University Press: New York, 1992.
(13) Kneller, G. R.; Doster, W.; Settles, M.; Cusak, S.; Smith, J. C. *J. Chem. Phys.* **1992**, *97*, 8864.
(14) Dianoux, A. J.; Kneller, G. R.; Sauvajol, J. L.; Smith, J. C. *J. Chem. Phys.* **1993**, *99*, 5586.
(15) See, e.g.: Sears, V. F. *Neutron News* **1992**, *3*, 26.
(16) Saelee, C.; Nicholson, T. M.; Davies, G. R. *Macromolecules* **2000**, *33*, 2258.
(17) See, e.g.: Mark, J. E., Ed.; *Physical Properties of Polymers Handbook*; AIP Press: New York, 1996.
(18) Prager, M.; Heidemann, A. *Chem. Rev.* **1997**, *97*, 2933.
(19) Zorn, R., private communication.
(20) Moreno, A.; Alegría, A.; Colmenero, J., to be published.
(21) Smith, G. D.; Boyd, H. *Macromolecules* **1992**, *25*, 1326.

MA9919256